iJRASET
International Journal For Research in Applied Science and Engineering Technology

# INTERNATIONAL JOURNAL FOR RESEARCH

IN APPLIED SCIENCE & ENGINEERING TECHNOLOGY

**Volume:** 5 **Issue:** XII **Month of publication:** December 2017

**DOI:**

www.ijraset.com

Call: 08813907089 | E-mail ID: ijraset@gmail.com

International Journal for Research in Applied Science & Engineering Technology (IJRASET)
*ISSN: 2321-9653; IC Value: 45.98; SJ Impact Factor:6.887*
*Volume 5 Issue XII December 2017- Available at www.ijraset.com*

# Automatic Skull Stripping using Maxima-Minima value from Quadratic Equations for MR Images

Siva Shankar R[1], Somasundaram K[2]
[1] *Department of Computer Applications, Madanapalle Institute of Technology & Science Angallu, Madanapalle-517325,Andhra Pradesh,*
[2] *The Gandhigram Rural Institute – Deemed University, Gandhigram, Tamil Nadu – 624302, India.*

***Abstract*: *Magnetic Resonance Imaging (MRI) is a significant imaging technique for studying various organs of a human, particularly of brain structure. Extraction of brain portion from MRI is needed by a physician, to study about the structure and to diagnose the diseases. This process is also known as skull stripping. Skull stripping process may be a manual, semi-automatic or fully automatic. Fully automatic methods are fast and extract the brain region from MRI more accurately. This paper presents the skull stripping method which makes use of quadratic equations and region growing for extracting the brain portion. Using quadratic equation, we find the maxima and minima value and to find brain boundary region growing is done at the coordinates where maxima and minima value found. We use 20 volumes of T1 coronal data sets and five volumes of T1 axial datasets. The proposed method gives average value of Jaccard coefficient, 0,9795, and Dice , 0.9797. The results show that our method can extract brain from MRI which are comparable to that of existing methods.***
***Keywords*: *MRI, skull stripping, maxima, minima, quadratic equation, region growing***

## I. INTRODUCTION

MR images of the brain give the anatomy of brain that is helpful to diagnose the brain related diseases[1]. It is taken in different relaxation times and shows variations in image intensity. Because, brain is composed of different tissue characteristics such as water, air, protein, fat etc. For better diagnosing, neurologist need segmented brain portion from MRI. Manual segmentation of brain by radiologists is time-consuming, inconsistent and also affected by operator bias. The computer assisted segmentation of brain helps to improve the speed and accuracy of diagnostic procedures in medical applications. Such segmentation process is referred as Skull Stripping or Brain Extraction. It is an important pre-processing technique in MRI. Brain Extraction Tool (BET)[2] is a popular skull stripping method. It employs deformable model that evolves to fit the brain's surface by the application of a set of locally adaptive model force. This method adds few non-brain tissues in the final segmented brain images.

Brain extraction can be achieved by region based and contour based methods. Several brain extraction methods[3-7] based on region growing, watershed and mathematical morphology are used to extract the brain portion from T1-w scans and T2-w scans separately. Region based methods view brain regions as a group of connected pixel data sets. These regions will have muscles, tissues, cavities, skin, optic nerves, etc. Contour based segmentation method is given by Somasundaram et al.[8] and this method extracts the brain regions accurately in T1-w, T2-w, and proton density–weighted normal and abnormal brain images. A **recent** skull stripping method[9] has been developed to extract brain portion from T1-w images, based on grayscale transformation and morphological operations. Few algorithms appear to have produced accurate results for both T1 and T2 weighted MR images[10-13]. All these methods have strength and weakness. Hence, we set our goal to develop a fully automatic tool to extract the brain portion both from T1and T2 head scans.

In this article, we propose a fully automatic skull stripping method using modified k-mean clustering and piecewise continous quadratic basis function. Experiments using the proposed method on 20 volumes of T1-w data sets and 5 volumes of T2-w data sets show that the proposed method gives better results than that of BET method. The remaining part of the article is organized as follows. In section 2, Materials and Methods are given. In section 3, Results and Discussion are given. Finally, Conclusion is given in section 4.

## II. BASIC PRINCIPLES USED

### *A. Turning Points*

The values used in mathematics are represented by variables and the functions which are used to describe the ways in which these variables change. Any turning points produces the ups and downs by the function which refers as its maximum and minimum. If we

want to know the precise location of such points we need to turn to algebra and differential calculus. Figure 1 shows such Turing points by the function f(x) [13]. If, at the points marked A, B and C, we draw tangents to the graph, note that these are parallel to the x axis. They are horizontal. This means that at each of the points A, B and C the gradient of the graph is zero.

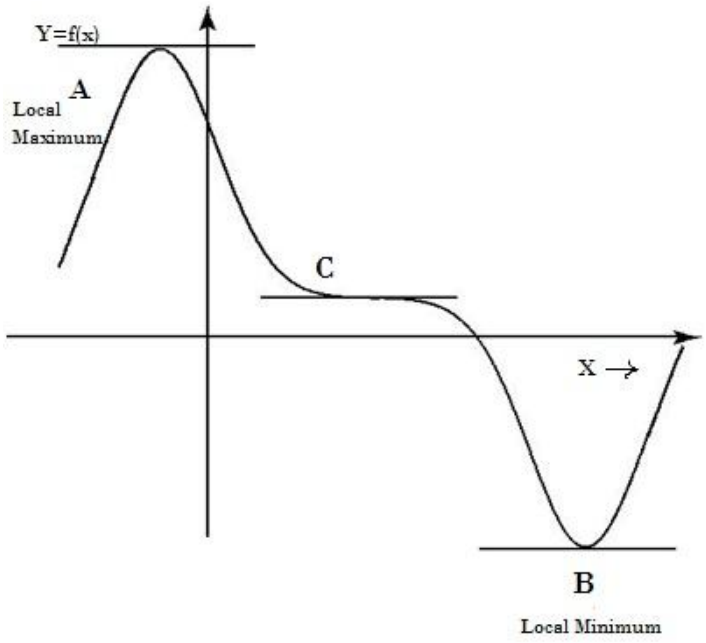


Figure1. The gradient of this graph is zero at each of the points A, B and C

We know that the gradient of a graph is given by $\frac{d_y}{d_x}$ consequently, $\frac{d_y}{d_x}$ = 0 at points A, B and C. All these points are known as stationary points. At points A and B the curve actually turns. These two stationary points are referred to as turning points. Point A in Figure 1 is called a local maximum because in its immediate area it is the highest point, and so represents the greatest or maximum value of the function. Point B in Figure 1 is called a local minimum because in its immediate area it is the lowest point, and so represents the least, or minimum, value of the function.

## III.METHODS AND MATERIALS

### *A. Fixing the Edges*

In MRI head scan images, the gray scale image properties are having intensity values from 0 to 255. The skull portions have the maximum intensity values and look merely white. Brain tissues have the highest value and also few gray shades among it. The region between edge of the brain portion and the skull will be having the possible combinations of maximum intensity value and minimum intensity value in all the slices in a dataset. We used the maxima minima properties from the turning points of quadratic equation as our processing technique.

The general form of the quadratic equation is:

$$y = ax^2 + bx + c \quad (1)$$

But we use the vertex form of the quadratic equation [14], [15] as

$$y = a(x-h)^2 + k \quad (2)$$

We make use this equation for an image as:

$$py = (px - ph)^2 + pk \quad (3)$$

where, px is the intensity value in each pixel, ph is the highest intensity value of the input image. pk is a constant positive value. py is the value to find the maximum or minimum values. We do this in the mid row of mid slice of the MR head scan volume. py

values denotes the property of gradient. When value of py starts decreasing, we can fix that the place of the turning point is as Maxima value. Then to find the Minima value by gradient flow, we trace the value of py where it starts growing upwards. We fix that the point turning as Minima value.

The edge of the brain portion will have the combination of the peak intensity values and lower value for CSF, such properties are reflected by maxima and minima values described above. This process helps to find the co-ordinate points of the edges of the brain portion in the MRI head scan images.

The occurrence of immediate maxima and minima values indicate the edges of brain, skull and sometimes tumors also. Some noisy images will also give its spurious edges. To avoid such spurious edges, we start the process from midpoint of the image by tracing maxima-minima point. If maxima-minima point is found, we apply region growing process. To trace or to fix the curve such as continuous edge with similar property, we use region growing process by using intensity similarity property between the current maxima minima point and the neighbour pixels at (x+i, y+j) where i and j ranges from -3 to 3. If intensity of current maxima-minima pair is equal to the intensity of neighbourhood pixels which also satisfies maxima-minima principle, then we mark both pairs as belonging to the same region. The growing process stops when no maxima - minima pair is found. The output of this region growing gives brain boundary. The region growing process is shown in Figure 2. The maxima element is given by (x, y) co-ordinate value and the remaining are neighbourhood pixels considered for region growing.

| | | | | | | |
|---|---|---|---|---|---|---|
| (x-3,y-3) | (x-3,y-2) | (x-3,y-1) | (x-3,y) | (x-3,y+1) | (x-3,y+2) | (x-3,y+3) |
| (x-2,y-3) | (x-2,y-2) | (x-2,y-1) | (x-2,y) | (x-2,y+1) | (x-2,y+2) | (x-2,y+3) |
| (x-1,y-3) | (x-1,y-2) | (x-1,y-1) | (x-1,y) | (x-1,y+1) | (x-1,y+2) | (x-1,y+3) |
| (x,y-3) | (x,y-2) | (x,y-1) | **(x,y)** | (x,y+1) | (x,y+2) | (x,y+3) |
| (x+1,y-3) | (x+1,y-2) | (x+1,y-1) | (x+1,y) | (x+1,y+1) | (x+1,y+2) | (x+1,y+3) |
| (x+2,y-3) | (x+2,y-2) | (x+2,y-1) | (x+2,y) | (x+2,y+1) | (x+2,y+2) | (x+2,y+3) |
| (x+3,y-3) | (x+3,y-2) | (x+3,y-1) | (x+3,y) | (x+3,y+1) | (x+3,y+2) | (x+3,y+3) |

Figure 2. Neighbourhood pixels considered for region growing about the current maxima-minima point(x,y)

*B. Extraction of the Brain portion in the Middle Slice*

The mid slice in the MRI volume contains the largest single portion as brain. It is easy to extract brain from that slice. Therefore we start the process from the middle slice of the given MRI volume. We apply the curve fitting by quadratic equations to find the maxima minima values. We first start the brain portion extraction in the middle slice for each brain volume, at approximately (W/2)th position, where W is the total number of slices in the volume. The mask for extracting the brain in the middle slice is used as reference. Our process will move from the middle slice to lower slices (LS) and then from middle slice to upper slices (US), one direction at a time.

At each slice, the mask of the brain for the previous slice will be used as reference to extract the brain in the current slice. This makes our process robust and reliable. The flow chart of our method is shown in Figure 3.

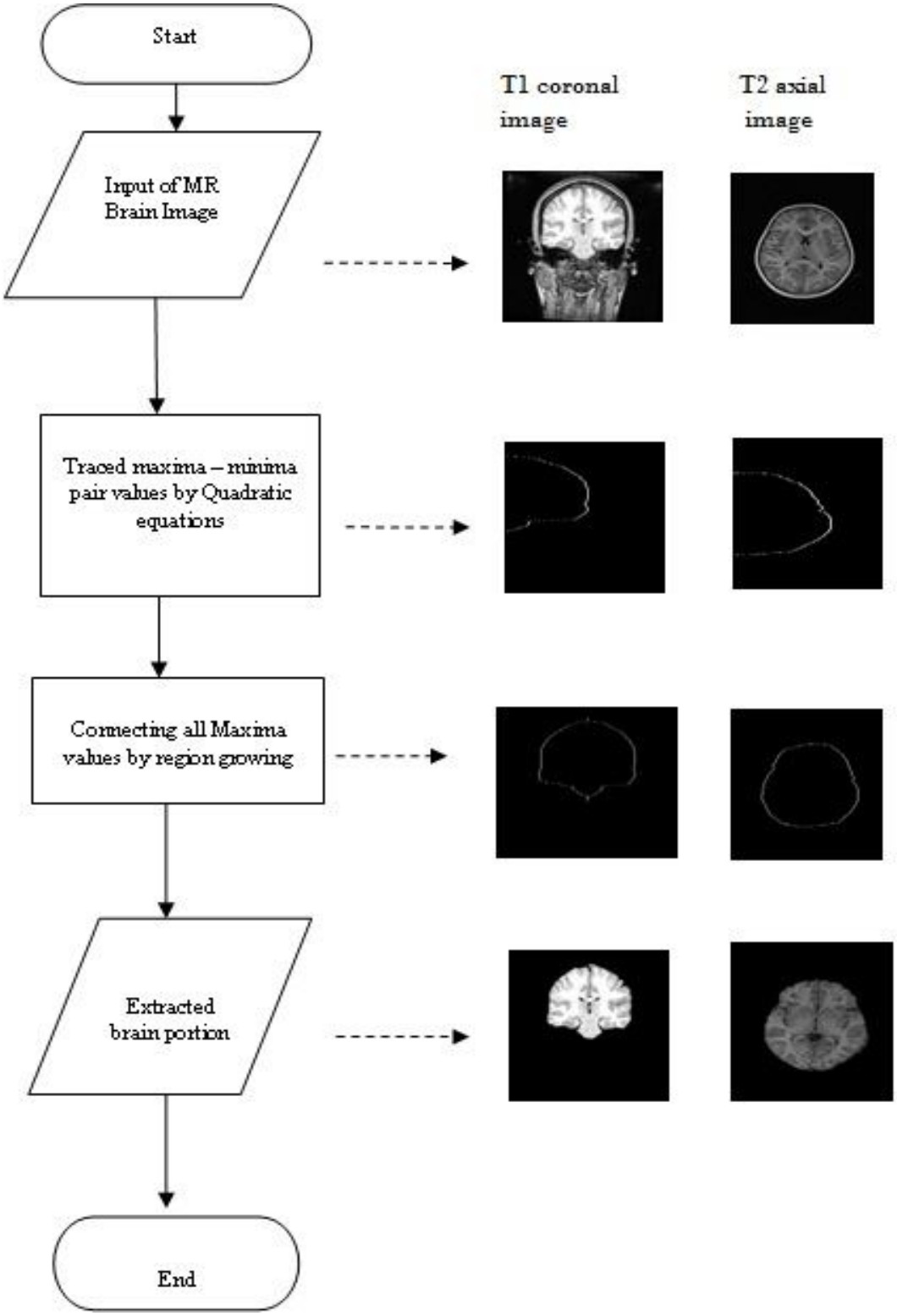


Figure3. Flow chart of the proposed method

*C. Performance evaluation metrics*

We make use of the following parameters to evaluate the performance of the proposed segmentation method. Several popular quantitative measures are available for comparing structural similarities of two images. Jaccard coefficient (J) and Dice coefficient

(D) are such measurements of asymmetry information on binary regions A and B.

The Jaccard coefficient [18] is given by:

$$J(A,B) = \frac{A \cap B}{A \cup B} \tag{4}$$

The Dice coefficient [19] is given by:

$$D(A,B) = \frac{2|A \cap B|}{|A| + |B|} \tag{5}$$

where, A and B are two data sets. The values of J and D varies from 0 for complete disagreement to 1 for complete agreement, between A and B.

The sensitivity (Sn) and specificity (Sp) are estimated between the hand segmented result by experts and the corresponding portions produced by the proposed automatic methods. The sensitivity (Sn) [20] is the percentage of ROI voxels recognized by an algorithm and specificity (Sp) [20] is the percentage of non-ROI voxels recognized by an algorithm. Sn and Sp are computed using the True Positive (TP), False Positive (FP), True Negative (TN) and False Negative (FN) values extracted by an algorithm.

$$S_n = \frac{TP}{TP + FN} \tag{6}$$

$$S_p = \frac{TN}{TN + FP} \tag{7}$$

The predictive accuracy (PA) [21] is the percentage of both ROI and non-ROI regions recognized by the proposed methods. TP and FP are the total number of pixels correctly and incorrectly classified as ROI by the automated algorithm. TN and FN are defined as the total pixels correctly and incorrectly classified as non-ROI tissue by an automated algorithm. PA is computed using:

$$PA = 100 \times \frac{TP + TN}{TP + TN + FP + FN} \tag{8}$$

Finally, false positive rate (FPR) and false negative rate (FNR) are used to measure the misclassification done by an algorithm. FPR is the number of voxels incorrectly classified as ROI by the automated algorithm and is given by:

$$FPR = \frac{FP}{TP + FN} \tag{9}$$

$$FNR = \frac{FN}{TP + FN} \tag{10}$$

*D. Materials Used*

We used twenty volumes of MRI T1 coronal datasets obtained from IBSR [16] website developed by Centre for Morphometric Analysis (CMA) at Massachusetts General Hospital, for the proposed method. The manually segmented brain images are also available at IBSR for these twenty volumes. We have also used five volumes of T1 axial MRI data sets collected from Meenakshi Mission Hospital, Madurai [17] and no gold standard is provided for this dataset.

Refer real paper, Its given as taken from IBSR and Dindigul scans

## IV. RESULTS AND DISCUSSIONS

We carried out experiments on the material pool. First, the qualitative evaluation of the performance of the method is assessed by visual inspection of the extracted brain. Figure 4 shows one volume of IBSR dataset and the brain portion extracted from the slices shown in Figure 4 are shown in Figure 5.

*ISSN: 2321-9653; IC Value: 45.98; SJ Impact Factor:6.887*
*Volume 5 Issue XII December 2017- Available at www.ijraset.com*

Figure 4. The original MRI slices of volume 7_8 [16]

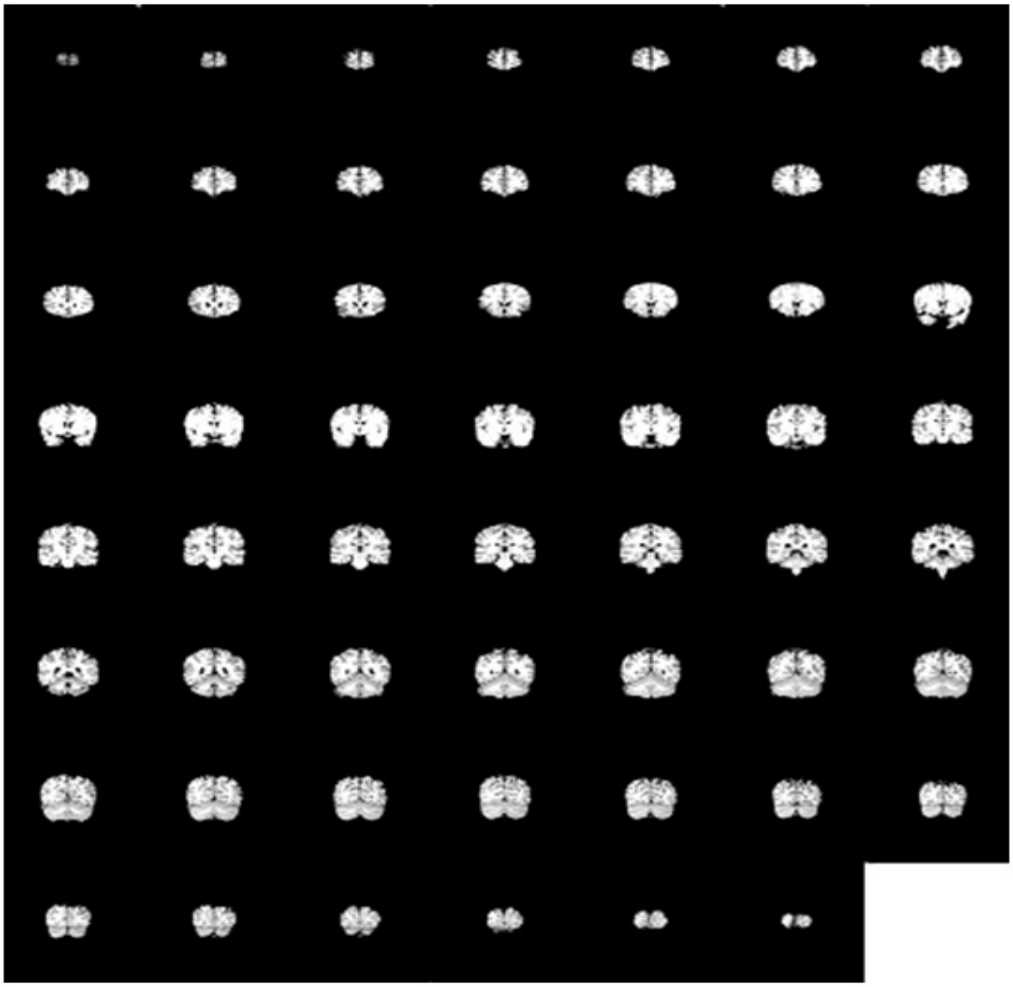

Figure 5. Extracted brain portion from slices in Figure 4

From Figure 5, we observe that the brain portions from all the slices are extracted properly. There are certain slices in which BET method failed to extract the brain portion. But our method performed well on these slices also. Figure 6 shows few slices where BET method failed and our method extracted the brain properly. First row, of Figure 6 shows the original slices, the second row shows the results obtained by BET and the third row by the proposed method.

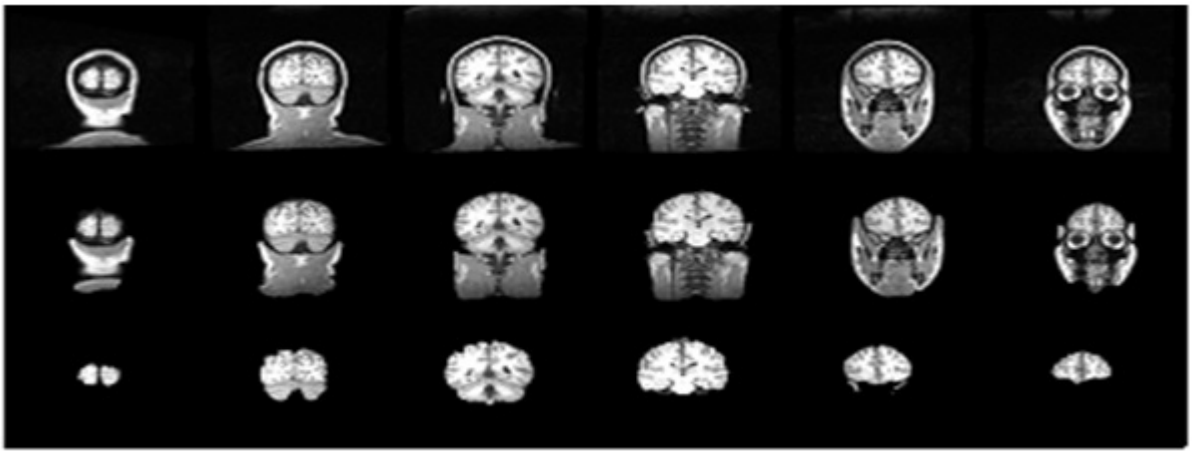

Figure 6. Row 1 shows the original image, row 2 shows the extracted brain portion by BET, row 3 shows the extracted brain portion by proposed method using coronal datasets collected from IBSR [16]

For quantitative evaluation, we computed the values of Jaccard coefficient (J)[18] and Dice coefficient (D)[19], false positive rate (FPR), false negative rate (FNR), sensitivity (Sn), specificity (Sp)[20], predictive accuracy (PA)[21] using equations (4) to (10) and are shown in Table 1. The mean values of these parameters are shown in Table 2 along the results obtain by BET [3] and BSE [4].

Table 1. Average value of J,D, Sn, Sp, FPR, FNR and TMR for 20 datasets

| S.No. | Vol. Label | J | D | Sn | Sp | FPR | FNR | TMR |
|---|---|---|---|---|---|---|---|---|
| 1 | 1_24 | 0.9911 | 0.9967 | 0.9978 | 0.9412 | 0.0065 | 0.0012 | 0.0077 |
| 2 | 2_4 | 0.9884 | 0.9952 | 0.9989 | 0.8770 | 0.0101 | 0.0011 | 0.0112 |
| 3 | 4_8 | 0.9776 | 0.9858 | 0.9994 | 0.7757 | 0.0222 | 0.0006 | 0.0228 |
| 4 | 5_8 | 0.9658 | 0.9855 | 0.9994 | 0.6587 | 0.0355 | 0.0006 | 0.0361 |
| 5 | 6_10 | 0.9619 | 0.9822 | 0.9992 | 0.6946 | 0.0400 | 0.0008 | 0.0408 |
| 6 | 7_8 | 0.9896 | 0.9969 | 0.9987 | 0.9132 | 0.0090 | 0.0013 | 0.0103 |
| 7 | 8_4 | 0.9876 | 0.9836 | 0.9981 | 0.8963 | 0.0020 | 0.0019 | 0.0039 |
| 8 | 11_3 | 0.9865 | 0.9854 | 0.9900 | 0.9873 | 0.0031 | 0.0010 | 0.0041 |
| 9 | 12_3 | 0.9826 | 0.9895 | 0.9853 | 0.9795 | 0.0036 | 0.0144 | 0.0180 |
| 10 | 13_3 | 0.9846 | 0.9852 | 0.9864 | 0.9900 | 0.0019 | 0.0136 | 0.0155 |
| 11 | 15_3 | 0.9446 | 0.9623 | 0.9997 | 0.5275 | 0.0590 | 0.0003 | 0.0593 |
| 12 | 16_3 | 0.9878 | 0.9733 | 0.9990 | 0.8729 | 0.0120 | 0.0010 | 0.0130 |
| 13 | 17_3 | 0.9925 | 0.9559 | 0.9984 | 0.9383 | 0.0064 | 0.0016 | 0.0080 |
| 14 | 100_23 | 0.9897 | 0.9756 | 0.9957 | 0.9527 | 0.0062 | 0.0043 | 0.0105 |
| 15 | 110_3 | 0.9889 | 0.9675 | 0.9903 | 0.9885 | 0.0017 | 0.0057 | 0.0074 |
| 16 | 111_2 | 0.9898 | 0.9876 | 0.9928 | 0.9760 | 0.0036 | 0.0072 | 0.0108 |
| 17 | 112_2 | 0.9916 | 0.9877 | 0.9927 | 0.9896 | 0.0015 | 0.0073 | 0.0088 |
| 18 | 191_3 | 0.9949 | 0.9865 | 0.9967 | 0.9622 | 0.0041 | 0.0033 | 0.0074 |
| 19 | 202_3 | 0.9579 | 0.9568 | 0.9999 | 0.5503 | 0.0673 | 0.0001 | 0.0674 |
| 20 | 205_3 | 0.9370 | 0.9553 | 0.9997 | 0.5635 | 0.0715 | 0.0003 | 0.0718 |
| | Avg. | 0.9795 | 0.9797 | 0.9959 | 0.8518 | 0.0184 | 0.0034 | 0.0218 |

Table 2. Average values of quantitative measures for our method, BET and BSE

| Method | J | D | Sn | Sp | FPR | FNR | TMR |
|---|---|---|---|---|---|---|---|
| BET | 0.7622 | 0.8619 | 0.9982 | 0.9155 | 0.8780 | 0.0030 | 0.8810 |
| BSE | 0.8883 | 0.8619 | 0.8856 | 0.9912 | 0.0860 | 0.1150 | 0.2010 |
| Proposed | 0.9795 | 0.9797 | 0.9959 | 0.8518 | 0.0184 | 0.0034 | 0.0218 |

From Table 2, we note that our method have produced highest J, 0.9795, and D, 0.9797, than BET and BSE methods. BET produces highest sensitivity, 0.9982, and BSE produces highest specificity, 0.9912, than our method. The sum of FPR and FNR (TMR=FPR+FNR) for BET is highest than our method and BSE. It implies that it includes several non brain tissues considering as brain region. But the total misclassification rate (TMR) should be as low as possible for segmentation method. Our method gives such lowest value, 0.0218, implying that it is the better than BET and BSE with low errors.

Figure 7 and Figure 8 shows the plot of average Jaccard and Dice coefficient for the 20 datasets. The labels along x-axis are the names of the IBSR datasets. From Figure 7, we note that the average Jaccard value of BET is low for the datasets 6_10, 7_8, 15_3, 16_3 and 17_3 and for BSE, the Jaccard value is low for 5_8 and 6_10.

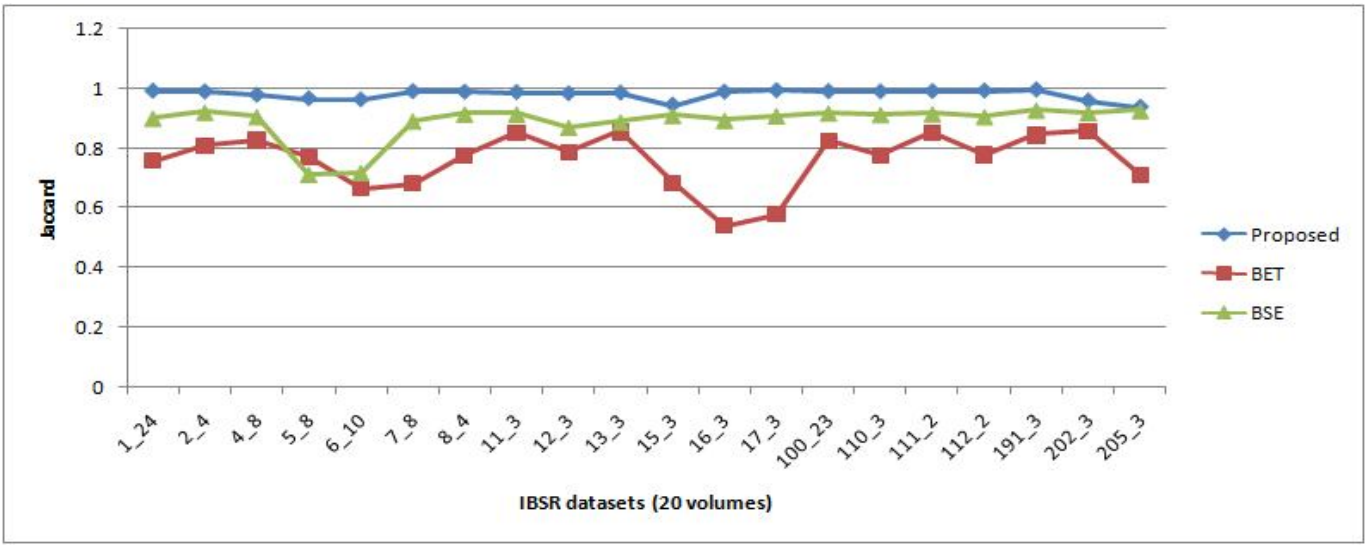


Figure 7. The average values of Jaccard(J) co-efficients computed for T1 volumes using the proposed method, BET and BSE

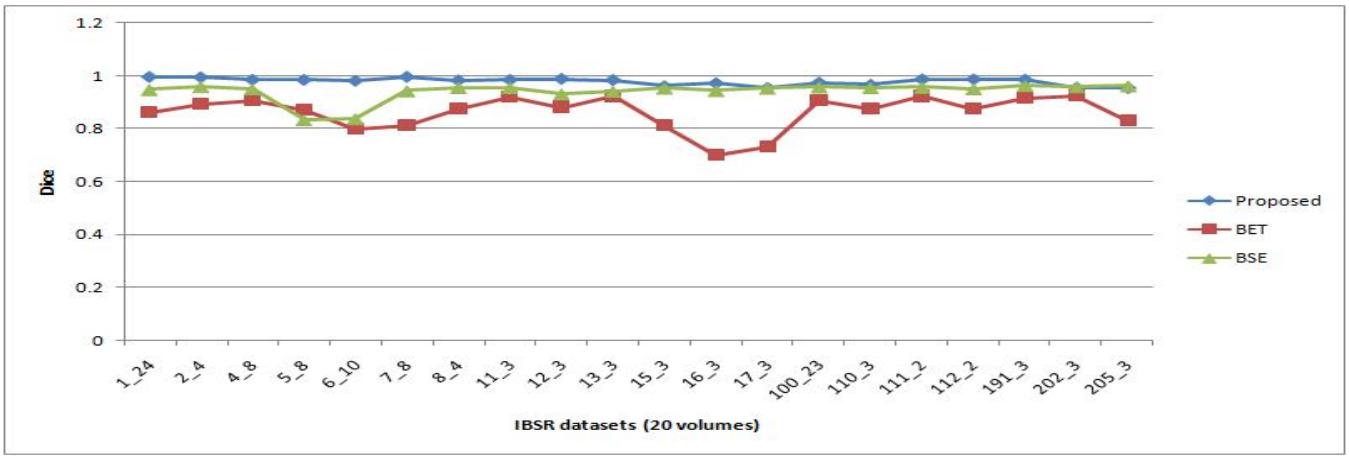


Figure 8. The average values of Dice (D) co-efficients computed for T1 volumes using the proposed method, BET and BSE

From Figure 8, we note that the Dice coefficient of BET is very low for the datasets 15_3, 16_3 and 17_3. The reason for this is either due to intensity non uniformity artifact among the datasets or the inability of the method to remove non-brain regions such as neck portion. The Dice value obtained by BSE is lower for datasets 5_8 and 6_10. BSE produced higher values of D for the dataset 205_3 than the proposed method.

We also carried out experiments on real data sets obtained from Meenakshi Mission Hospital, Madurai. The brain portions extracted from the volumes collected from Meenakshi Mission Hospital, Madurai, are shown in Figure 9 and the brain portion extracted from the slices shown in Figure 9 are shown in Figure 10.

There are no gold standard available for this set. The results of the automated brain extraction algorithm was visually analyzed by the several experts from radiology and neurology fields and confirmed that the results as adequate to further processing. Experimental results show that the proposed method correctly segments the whole brain completely by delineating the non-brain tissues. Hence, the performances of the proposed method is found to be better than the well known method BET. For visual inspection the original images and the extracted images by BET and our method are shown in Figure 11.

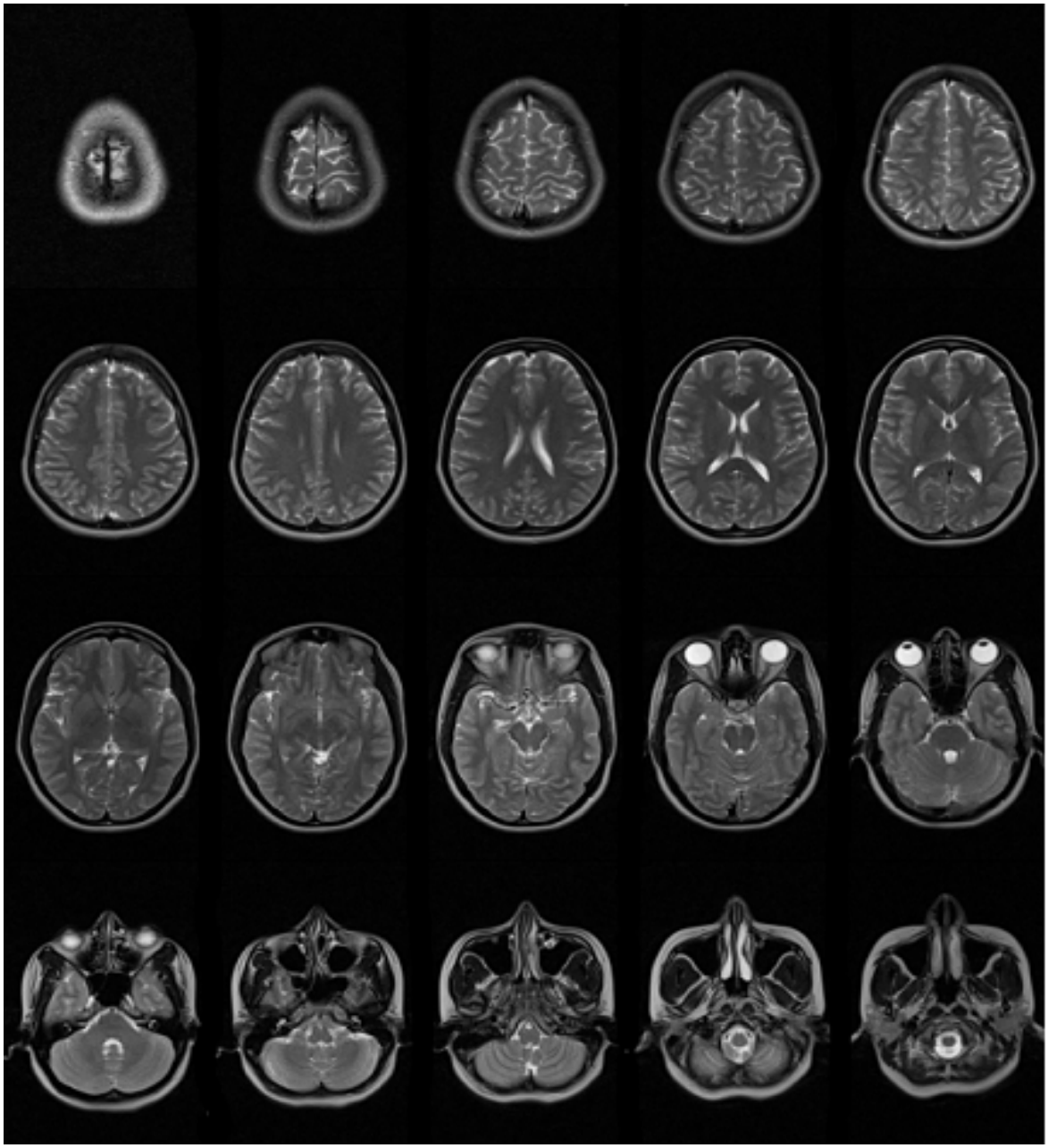

Figure 9. Sample volume of original MRI slices collected from MMH[17].

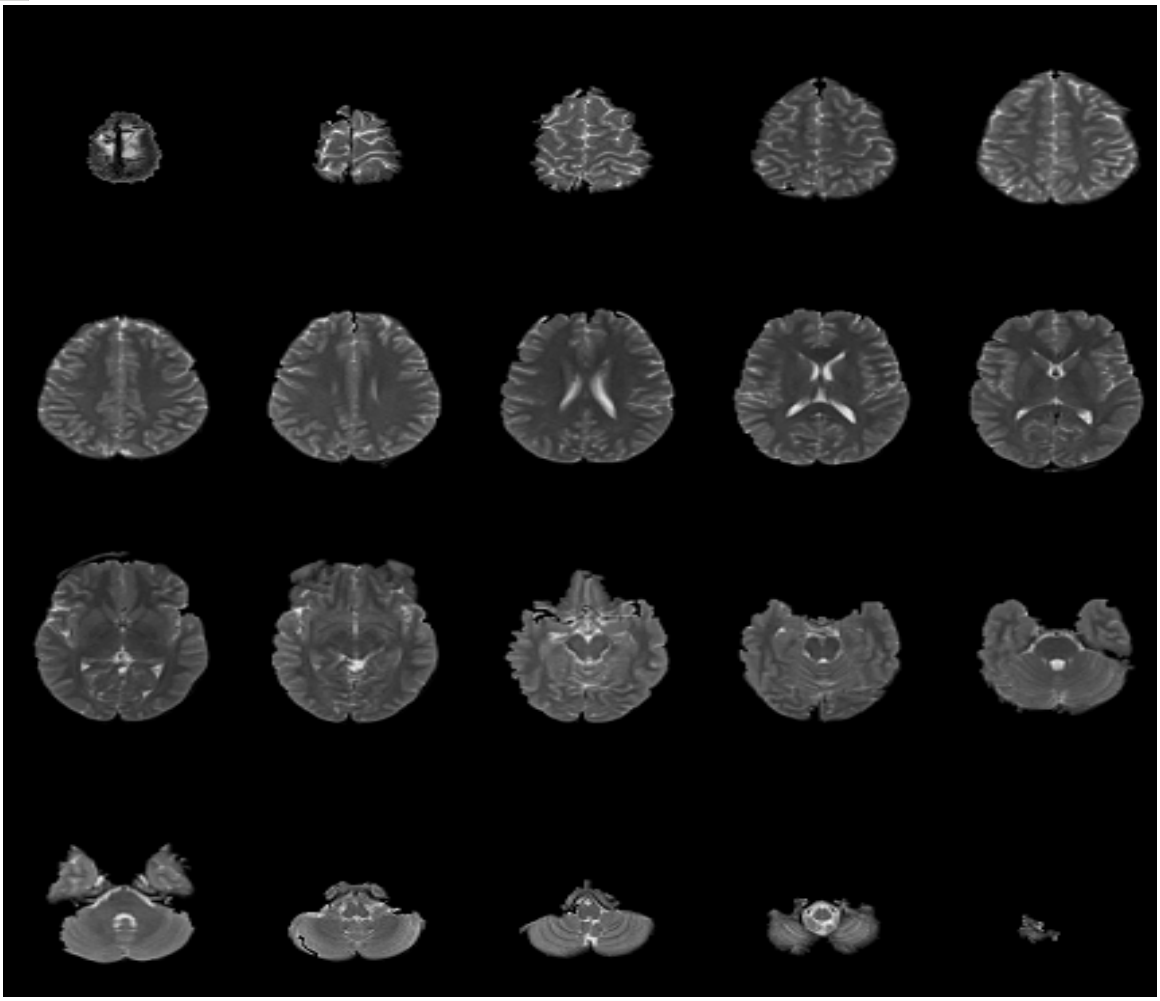

Figure10. Extracted brain portion from slices in Figure 9

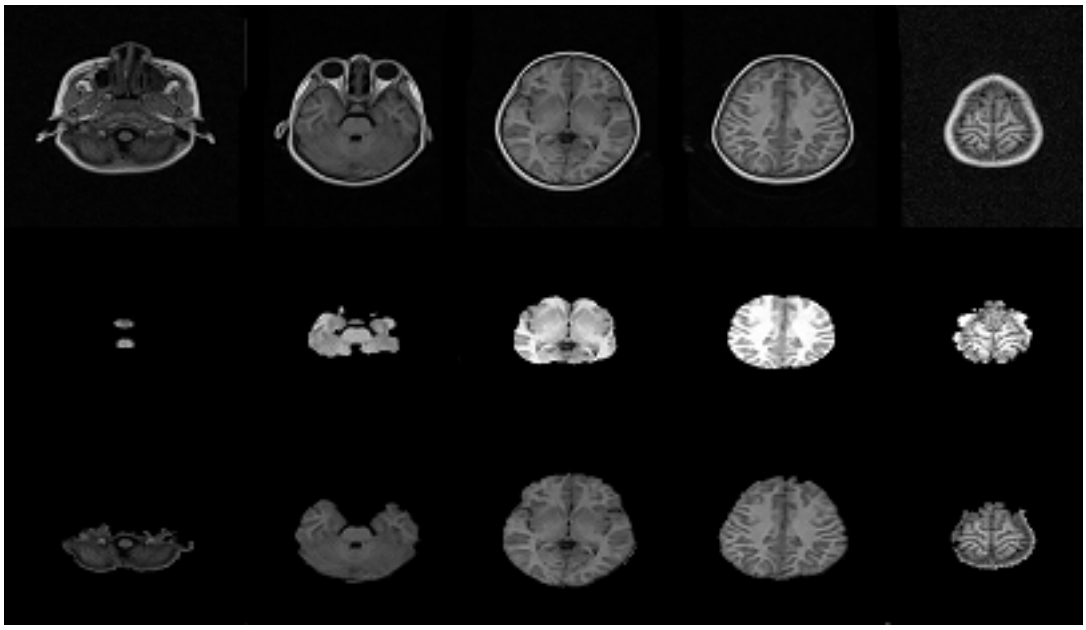

Figure 11. Original slices are shown in first row and the extracted brain by BET (row2) and by our method (row 3) using datasets collected from MMH[17].

## V. CONCLUSION

In this paper we have proposed a novel method to extract brain portion from MRI human head scan images. The proposed scheme is based on quadratic equations and region growing. Our method is able to detect the boundary to separate brain portion and skull directly from T1 coronal and T2 axial MR images and thus avoids the pre-processing to remove background and skull areas. The proposed method gives better result in terms of the Jaccard and Dice similarity indices than BET and BSE.

## VI. ACKNOWLEDGEMENT

The authors would like to acknowledge Dr.Karunakaran., MBBS., DMRD., DNB(RD) Radiologist, Department of Imaging and Interventional Radiology, Meenakshi Mission Hospital and Research Centre, Madurai-625107., and Dr.K.G.Srinivasan., M.D., RD., Radiologist KGS Advanced MR & CT Scan, Madurai, Tamil Nadu, India., for giving suggestions and evaluating our segmented results.

## REFERENCES

[1] Habib Z, Marie L, Abass A. Clinical role on Fusion Imaging using PET, CT and MR Imaging. Magn Reson Imaging. 2010;18:133-149.
[2] Smith SM. Fast robust automated brain extraction. Hum Brain Mapp. 2002; 17:143–155.
[3] Somasundaram K, Kalaiselvi T. Automatic brain extraction methods for T1 magnetic resonance images using region labeling and morphological operations. Comp Bio Med. 2010;41:716–725.
[4] Mehdi J, Shohreh K. Automatic Brain Tissue Detection in MRI Images Using Seeded Region Growing Segmentation and Neural Network Classification. Aust J Basic & Appl Sci. 2011; 5:1066-1079.
[5] Orazio G, Enrico D, Matteo S, et al. Automatic Skull Stripping in MRI based on Morphological Filters and Fuzzy C-means Segmentation. 33rd Annual International Conference of the IEEE EMBS. 2011; 5040-5043.
**[6]** Galdames FJ, Jaillet F, Perez CA. An Accurate Skull Stripping Method Based on Simplex Meshes and Histogram Analysis in Magnetic Resonance Images. J Neurosci Methods. 2012; 2:103-119.
**[7]** Rosniza R, Nursuriati J, Rozi M. Skull Stripping Magnetic Resonance Images Brain Images: Region Growing versus Mathematical Morphology. IJCISIM. 2011; 3:150-158.
[8] Somasundaram K, Kalavathi P. Contour-Based Brain Segmentation Method for Magnetic Resonance Imaging Human Head Scans. J Comput Assist Tomogr. 2013; 37:353–368.
**[9]** Somasundaram K, Ezhilarasan K. Automatic Brain Portion Segmentation From Magnetic Resonance Images of Head Scans Using Gray Scale Transformation and Morphological Operations; J Comput Assist Tomogr.2015;39;552-558.
**[10]** Somasundaram K, Siva Shankar R. A novel Skull Stripping Method for T1 Coronal and T2 Axial Magnetic Resonance Images of Human Head Scans Based on Resonance Principle. International conference on Image Processing. Computer Vision and Pattern Recognition organized by WORLDCOMP'12, Las Vegas, Nevada, USA. 2012.
[11] Artem M, Gregory N, Siddharth G, et al. Fully Automatic Segmentation of the Brain From T1-Weighted MRI Using Bridge Burner Algorithm. J Magn Reson Imaging. 2008;27:1235-124.
[12] Zu YS, Guang HY, Jing ZL. Automated Histogram –Based Brain Segmentation in T1-Weighted Three-Dimensional Magnetic Resonance Head Images. NeuroImage. 2002;17:1587-1598.
[13] Sadananthan SA, Weili Z, Michael WL Chee. Skull Stripping using graph cuts. Neuroimage. 2010; 49:225-239.
[14] Internet Brain Segmentation Repository (IBSR). Available at: https://www.nitrc.org/projects/ibsr Center for Morphometric Analysis, Harvard University; downloaded on June 12 2012.
[15] SBC scans, Dindigul, State of Tamil nadu, India.
[16] Kofi PA . Some Basis Functions for Principal Fitted Components. University of Alabama at Birmingham. 2009.
[17] Sukumar N. Quadratic maximum-entropy serendipity shape functions for arbitrary planar polygons. Comput Methods in Appl Mech Eng.2013;263:27-41.
[18] Jaccard P. The distribution of flora in the alpine zone. New Phytol.1912;11:37–50.
[19] Dice L. Measures of the amount of ecologic association between species. Ecology. 1945;26:297–302.
[20] Altman DG, Bland JM. Statistics Notes: Diagnostic tests 1: sensitivity and specificity. BMJ.1994;308:1552.
[21] Devashish S, Yadav UB, Pulak S. The Concept of Sensitivity and Specificity in Relation to Two Types of Errors and its Application in Medical Research. JRSS. 2009;2:53-58.
[22] Meng L, Stanley Y, Hao W. Glioma Grading: Sensitivity, Specificity, and Predictive Values of Perfusion MR Imaging and Proton MR Spectroscopic Imaging Compared with Conventional MR Imaging. J Neuro Radiol. 2003; 24:1989-1998.
[23] Gary MG, Monica LG. Introduction to Biostatistics: Sensitivity, Specificity, Predictive Value and Hypothesis Testing. Ann Emerg Med. 1990; 591-596.

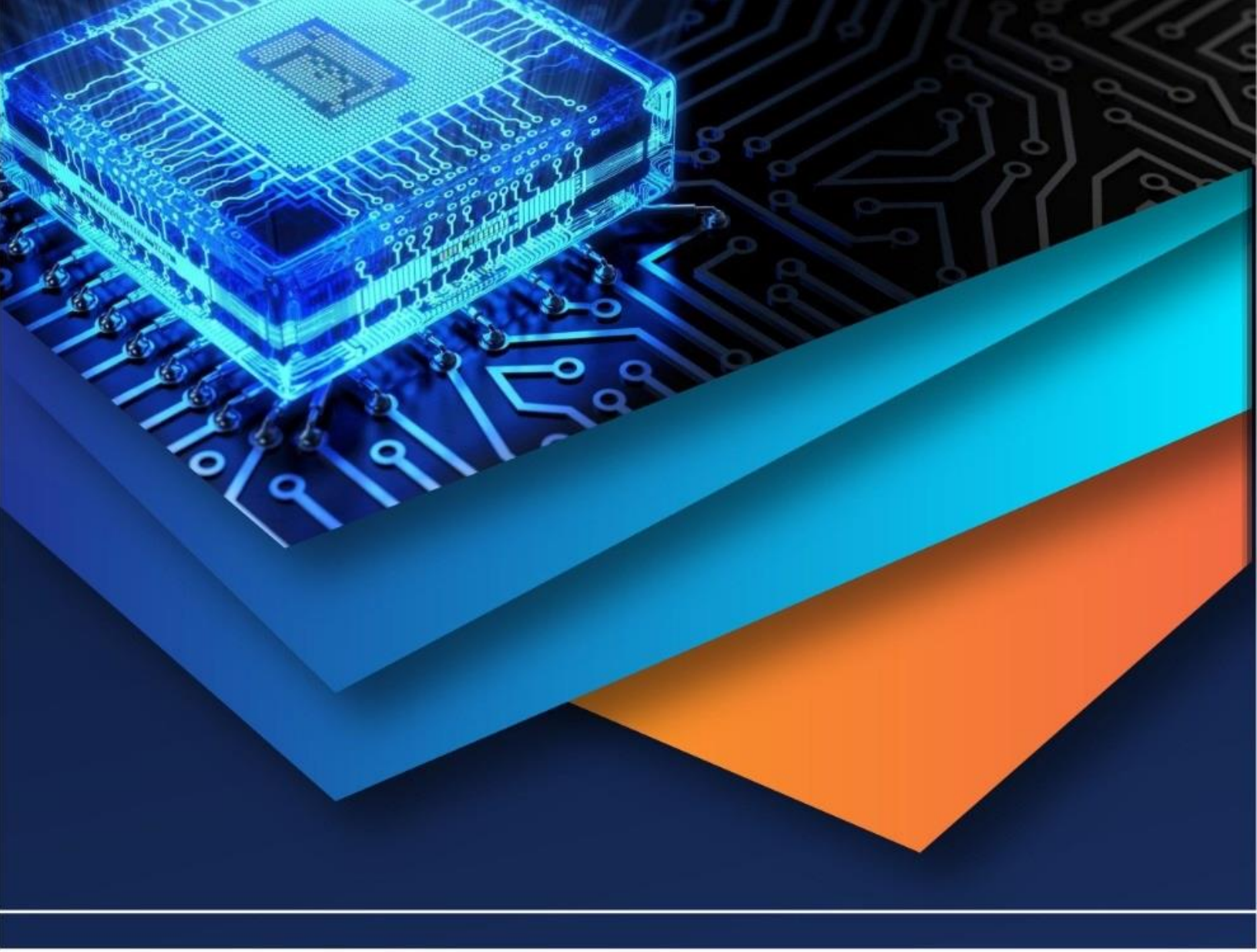

10.22214/IJRASET

45.98

IMPACT FACTOR: 7.129

IMPACT FACTOR: 7.429

# INTERNATIONAL JOURNAL FOR RESEARCH

IN APPLIED SCIENCE & ENGINEERING TECHNOLOGY